Continuing subsidence and deformation of the Surtsey volcano, Iceland

ERIK STURKELL[1*], PÁLL EINARSSON[2], HALLDÓR GEIRSSON[2], ÁSTA RUT HJARTARDÓTTIR[3], MD. TARIQUL ISLAM[4], JAMES G. MOORE[5], CHIARA LANZI[3], GUÐMUNDUR ÞÓR VALSSON[6] AND FREYSTEINN SIGMUNDSSON[2]

[1]Department of Earth Sciences. University of Gothenburg. Gothenburg. Sweden (erik.sturkell@gvc.gu.se)

[2]Institute of Earth Sciences. University of Iceland. Reykjavik. Iceland.

[3]Icelandic Meteorological Office, Reykjavík, Iceland

[4]Sab'a Sanabil Foundation, House 25, Road 3, Priyanka City, Uttara, Dhaka-1230, Bangladesh

[5]U.S. Geological Survey, Menlo Park, California, U.S.A.

[6]Natural Science Institute of Iceland, Akranes, Iceland

ABSTRACT

The Surtsey Island was built from 130 m water depth during the period 1963–1967. Two tephra cones formed above sea level reaching a height of 170 m a.s.l. The final surface area of Surtsey reached 2.65 km^2 with a volume of 0.8 km^3 (dense rock equivalent). Repeated levelling and Global Position System (GPS) campaigns have been carried out every 5–10 years to monitor the internal deformation and subsidence of the island. The first levelling measurements were made in the summer of 1967. Surtsey follows an exponentially decaying subsidence curve, with total subsidence reaching 1 m since 1967. The 2000–2023 GPS surveys confirmed that Surtsey moves horizontally with the Eurasian plate. The average subsidence rate for the three GPS monitoring sites during 2000-2023 was 3.8 mm/yr, a total of 9 cm. About 2/3 of the total subsidence is contributed by compaction of sedimentary and volcaniclastic material, thermal contraction, and palagonization. Up to 1/3 of the total subsidence can be explained by loading of the island on the asthenosphere.

INTRODUCTION

The Surtsey fires of 1963–1967 off the south coast of Iceland are one of the most significant volcanic episodes in Iceland in the twentieth century. A total of about 0.8 km^3 DRE (dense rock equivalent) of basaltic material erupted during the 3 ½ years of the activity. The course of Surtsey eruptive events has been described extensively (e.g., Thorarinsson *et al*. 1964, Thórarinsson 1965, 1967, Þórarinsson 1964, 1965, 1966, 1969, Einarsson 1966, Jakobsson *et al*. 2000). The submarine eruption was first detected on November 14, 1963, and the last sign of activity was observed in early June 1967 (Þórarinsson 1969). In a series of eruptions three islands were formed, only Surtsey survived the oceanic erosion. The activity attracted considerable attention in the scientific community, in connection with the newly proposed hypothesis of seafloor spreading with Iceland located on the mid-Atlantic spreading zone. The activity was conventionally defined as one, slightly discontinuous eruption (e.g., Thorarinsson *et al*. 1964, Þórarinsson 1964, 1965, 1966, 1967, 1969, Einarsson 1966). Later revision of available seismic data, and experience from subsequent episodes of volcanic activity in Iceland, e.g. the Krafla volcano-tectonic episode of 1975-1984 (Björnsson *et al.* 1977, Einarsson 1991, Einarsson & Brandsdóttir 2021) and the ongoing series of events on the Reykjanes Peninsula (e.g., Parks *et al.* 2025, Geirsson *et al.* 2024) has led to the general view that

the formation of Surtsey is better described as a series of at least six distinct eruptions fed from a single source (e.g., Sayyadi *et al.* 2021, 2022).

Prior to these events, the eruption site was a flat insular shelf at a depth of about 130 m (Jakobsson *et al*. 2000). The eruption site is the southernmost one within the Vestmannaeyjar volcanic system (VVS), the southernmost system within the Eastern Volcanic Zone of Iceland (EVZ) (Fig. 1). The volcanic zone extends south-westwards from the rift-transform junction of the EVZ with the South Iceland Seismic Zone (SISZ, Fig. 1). This part of the volcanic zone, sometimes called the South Iceland Volcanic Zone (SIVZ in Figure 1), has been interpreted as a propagating rift (e.g., Oskarsson *et al*. 1985, Meyer *et al*. 1985, Einarsson 1991), extending into the Eurasia Plate. Surtsey is located at the tip of this intraplate rift, where the rift propagation is driven by volcanic processes. Inter-plate tectonic motion is only observed across the EVZ and SISZ but currently not across the South Iceland Volcanic Zone, SIVZ. This is confirmed by recent GPS and InSAR measurements, showing that the nearby Heimaey, as well as the Eyjafjallajökull and Katla volcanoes also belong to the Eurasian plate (Geirsson *et al*. 2006, 2012, Árnadóttir *et al*. 2009, Cao *et al*. 2023).

The Vestmannaeyjar Volcanic System consists of several islands, the largest of which are Heimaey and Surtsey, and several seamounts (Sayyadi *et al.* 2024). Most of these are remnants of eruptions that began on the sea floor, and some of them reached the surface and formed lava flows. The competing processes of erosion by the sea and palagonitization of the tephra have subsequently shaped these structures. There are

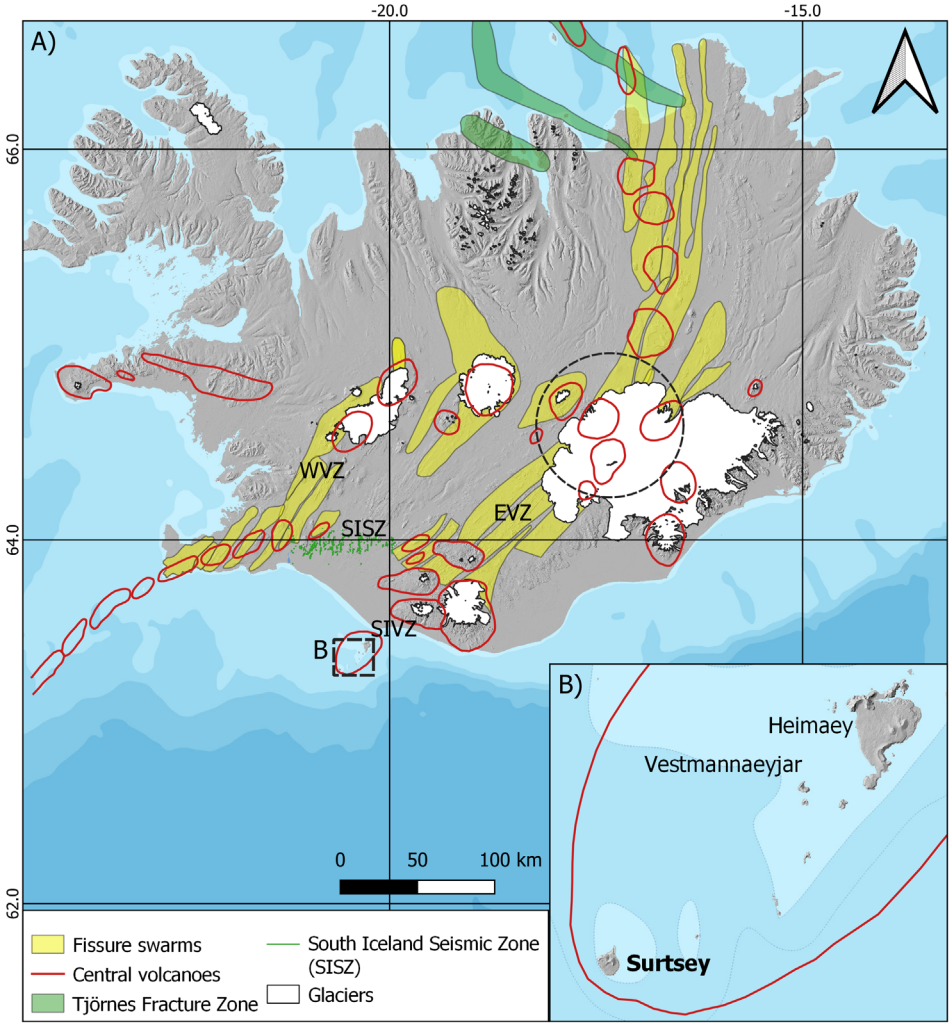

Figure 1. Map of Iceland showing the plate boundary and volcanic flank zones with Surtsey at the southernmost end. On the map, the Western Volcanic Zone (WVZ), the Eastern Volcanic Zone of Iceland (EVZ), the South Iceland Seismic Zone (SISZ) and the South Iceland Volcanic Zone (SIVZ) are marked. The centre of the Icelandic mantle plume is marked with a dashed circle with the Bardarbunga volcano in the centre.

no signs of normal faulting or graben structures in the Vestmannaeyjar archipelago, consistent with its intraplate location. Long term GPS measurements show that Vestmannaeyjar (GPS site VMEY) moves completely with the Eurasian plate (Geirsson *et al*. 2006). Eruptive fissures are mostly short and oriented NE-SW.

The 1963–1967 eruptions and the formation of Surtsey Island have been the subject of a multitude of scientific experiments, both in biology and geology. A significant mass of volcanic material was transferred from depth to the surface during the Surtsey eruptions. This mass is subject to internal evolution and furthermore has a mechanical effect on the underlying crust. Processes to be considered include elastic response of the lithosphere, isostatic adjustment, gradual compaction of loose materials, gravitational spreading of the edifice, lithification because of palagonitization, and erosion.

Ground deformation observations in Surtsey were initiated in 1967 when Tryggvason (1968) installed a levelling profile across the island. The profile has been re-measured several times and in 1992 it was connected to the GPS network in south Iceland (Einarsson *et al*. 1994). Sturkell *et al*. (2009) assembled all the levelling and GPS data on Surtsey obtained until 2002. In this paper, we summarize the results of previous measurements, as well as new measurements from 2013 and 2023, and evaluate the results with respect to deformation processes and recently acquired structural data from boreholes drilled in 2017 (Moore & Jackson 2020).

METHODS

Levelling

In 1967 a levelling line was installed across the new island consisting of 42 benchmarks cemented in bedrock (Tryggvason 1968) spaced approximately 50 m apart (Fig. 2). The erosive forces of the sea have shortened the original levelling line by 16 benchmarks. Several benchmarks have also been lost in the sand drift over the years. However, some have been re-exposed, and their coordinates determined by GPS measurements (prior to GPS, a theodolite and a geodimeter were used). All coordinates of the benchmarks prior to 2013 are tabulated in Sturkell *et al*. (2009) together with the raw data from the eleven levelling campaigns. The levelling from 2002 onwards is performed with a Zeiss Dini-12 levelling

Table 1. Data for the levelling performed across Surtsey in 1991, 2002, 2013, and 2023. Heights are given in meters relative to benchmark 606. For levelling data 1967–2002 see Sturkell *et al*. (2009).

Site	1991	2002	2013	2023
WP	-20.017			
605			-2.290	
606	0.000	0.000	0.000	0.0000
607	2.561	2.562	2.561	25.591
608			2.095	20.935
609	3.216	3.246	3.261	32.676
610				
611		7.890	7.924	79.430
612	10.096	10.156	10.191	102.091
613				
614				
615				
616		21.654	21.692	217.129
617		23.129	23.166	231.886
618			26.253	
619				
620				
621	30.374	30.414	30.435	304.454
622	31.399	31.450	31.477	314.916
623	31.583	31.638	31.668	316.783
624	32.629	32.689	32.720	327.306
625	35.064	35.122	35.143	351.264
626	34.035	34.089	34.094	340.224
627	25.876	25.920	25.883	
628	17.953	17.807		
629	11.282			
630	9.926			
510	-5.399	-5.386	-5.383	-53.924
511	-4.364	-4.364	-4.365	-43.641
512	41.860	41.929	41.966	419.846
513	46.471	46.539	46.578	465.966
514	50.184	50.248	50.283	502.935
515	50.831	50.892	50.925	509.402
516	50.653	50.714		
517	45.407	45.461	45.486	454.950
518	47.891	47.946	47.975	480.043
519	41.668	41.721	47.975	417.699
520	33.660	33.706	33.729	337.414
P-1	-15.130			
S-1	6.938			
S-2	14.613	14.678	14.717	147.380
S-3	20.974	21.049	21.090	211.124
S-4	37.117	37.184	37.221	372.386
S-6				
S-7	-15.989			
SDH-1	38.530			
SDH-2				
NE07*		14.251		
NE09		29.721	29.754	297.730
NE10		30.274	30.303	303.191
TW	29.229			

* Benchmark NE07 is in the centre of the helicopter platform (GPS SURP).

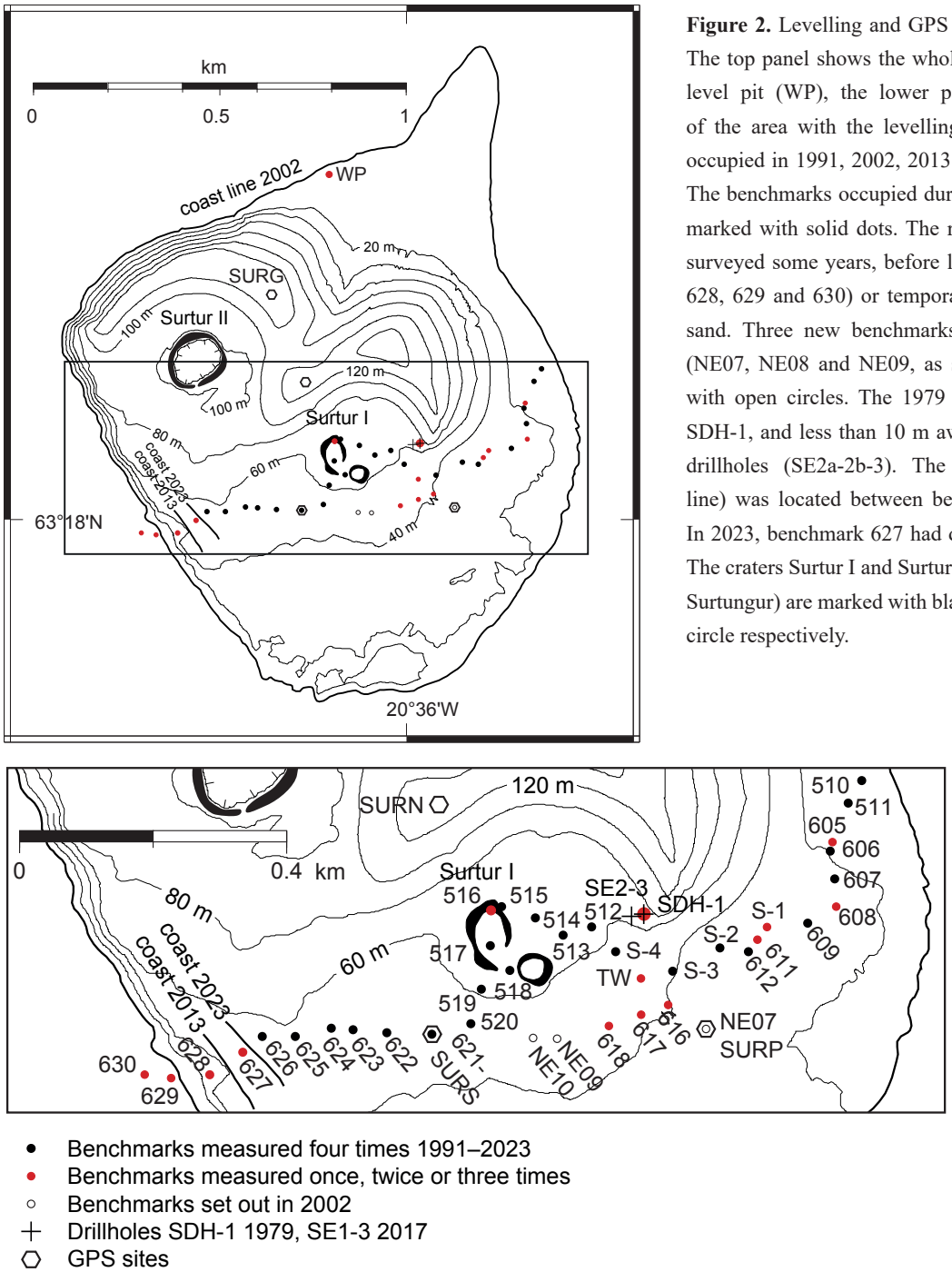

Figure 2. Levelling and GPS benchmarks on Surtsey. The top panel shows the whole island with the water-level pit (WP), the lower panel is an enlargement of the area with the levelling line. The benchmarks occupied in 1991, 2002, 2013 and 2023 (see Table 1). The benchmarks occupied during all these surveys are marked with solid dots. The red dots are benchmarks surveyed some years, before lost to the sea (WP, 627, 628, 629 and 630) or temporarily lost due to drifting sand. Three new benchmarks were set out in 2002 (NE07, NE08 and NE09, as shown on map) marked with open circles. The 1979 drill hole is located by SDH-1, and less than 10 m away from the three 2017 drillholes (SE2a-2b-3). The 2013 coastline (black line) was located between benchmarks 627 and 628. In 2023, benchmark 627 had disappeared into the sea. The craters Surtur I and Surtur II (usually referred to as Surtungur) are marked with black half circles and a full circle respectively.

instrument and two Zeiss levelling rods with digital barcodes which are read by the instrument (Fig. 3). The height difference between consecutive benchmarks is measured, and for redundancy the readings are repeated by swapping rods and re-setting the levelling instrument, until a difference of less than 0.20 mm is obtained between each reading, from which an average is calculated. Height of the benchmarks relative to any benchmark in the line can then be computed. The levelling results from 1991, 2002, 2013 and 2023 are given in Table 1 relative to benchmark 606, located on the east part of Surtsey (Fig. 2b).

To determine the absolute subsidence or uplift of Surtsey is a challenge because of the relative nature of levelling measurements and distance to the next island. Before the era of GPS, the height reference of the Surtsey levelling line was tied to the surface of a pond located by the northern shore of Surtsey (point WP in Fig. 2) that was initially assumed to represent mean sea level (Tryggvason 1968). However, as the water level in the pond was out of phase with the

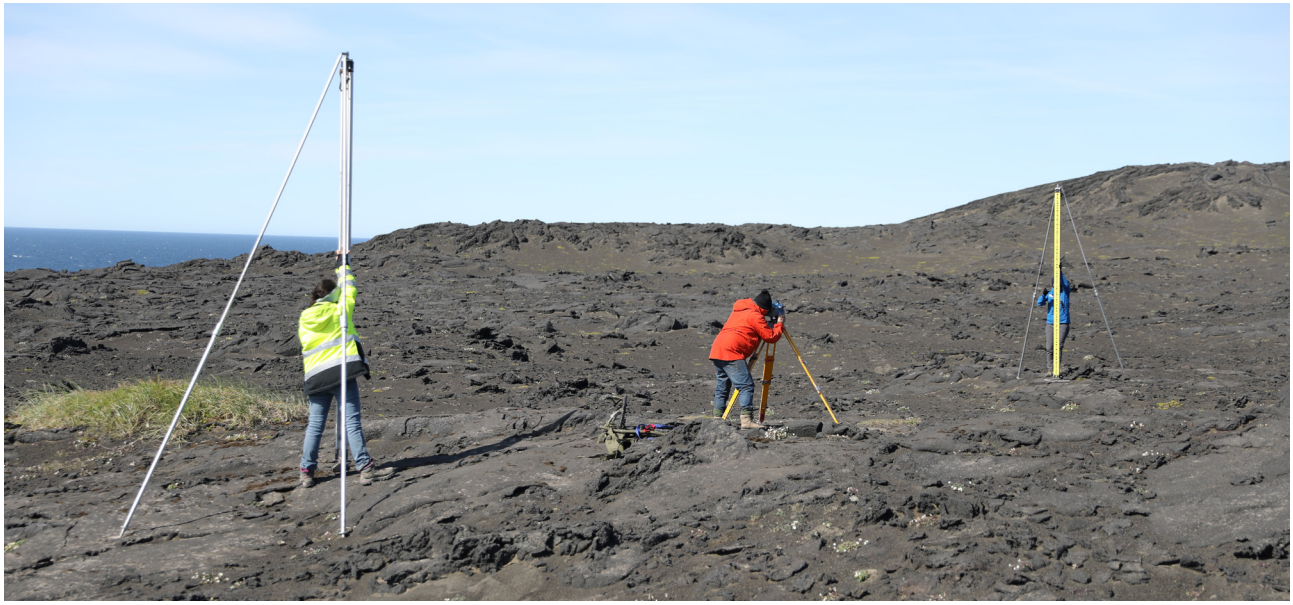

Figure 3. Levelling on Surtsey in 2023, the levelling instrument is located between the rods. The rod to the left is on a temporary benchmark to bridge between permanent benchmarks. The benchmark to the right is number 622. Photograph: Kristján Jónasson.

predicted ocean tide at Heimaey, it was considered to be somewhat higher than the sea level (Tryggvason 1968). The pond had disappeared in 1969, but as the groundwater table was close to the surface, a pit was dug to observe the water table (Tryggvason 1972). The water level in a dug pit corrected for the ocean tide was used as the datum for the levelling campaigns made in 1967 to 1991 (Moore *et al*. 1992, and references there in). Moore (1982) reported that in 1979 the best available estimate places the average water level in the dug pit at 32 ± 15 cm above the mean sea level. One of the benchmarks (SURS/621) has been occupied since 1992 as a GPS point (Fig. 4). The elevation of this benchmark relative to the water level in the dug pit or the water pit (WP), which was located 100 m east of the old northern cabin (see Section 4.2 for details), shows the exponentially decaying rate of the long-term absolute vertical movements.

The levelling in 1979 tied the drill hole top (SDH-1) and its water level (Moore *et al*. 1992) with the water-level pit (WP, Fig. 2). Benchmarks S-1 to S-7 were installed in 1979 and benchmarks 510 to 520 in 1982. Benchmarks 510 and 511 were installed to fill gaps in the original levelling line, and benchmarks 512 to 520 were laid out in a loop through the centre of the Surtur I crater. During the levelling in 2002 two new benchmarks (NE09 and NE10, Fig. 2) were installed along the line because benchmarks 618, 619 and 620 were not found that year.

GPS measurements

GPS campaigns were performed on Surtsey in 1992, 2000, 2002, 2013, 2017 and 2023. In 1992 SURS (same as BM 621, Fig. 2) was measured. In 2000 SURS and a new GPS-point (SURN) were measured. The description of the processing of the 1992, 2000 and 2002 data is given by Sturkell *et al*. (2009). In 2002 SURS and SURN were re-occupied and two new points added: One point in palagonite on the crest of the western mountain (SURG, inscription NE08); and the second point in the centre of the helicopter platform (SURP, inscription NE07, Fig. 2). The

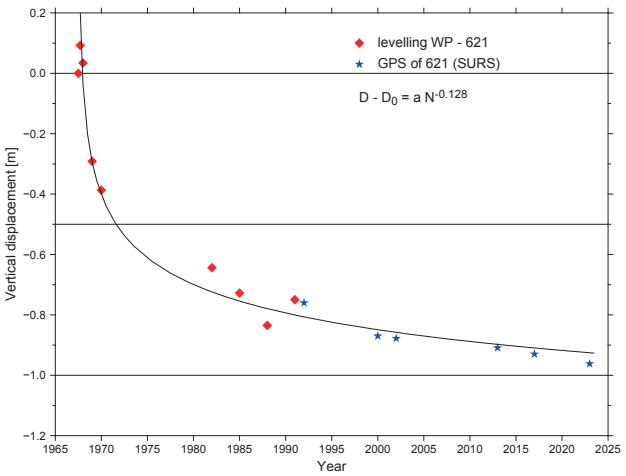

Figure 4. The vertical displacement between the water table in the dug pit (WP) and benchmark 621 from June 1967 to 1991, extended with GPS data for the site SURS (BM 621). The levelling and GPS data are presented in Tables 2 and 3.

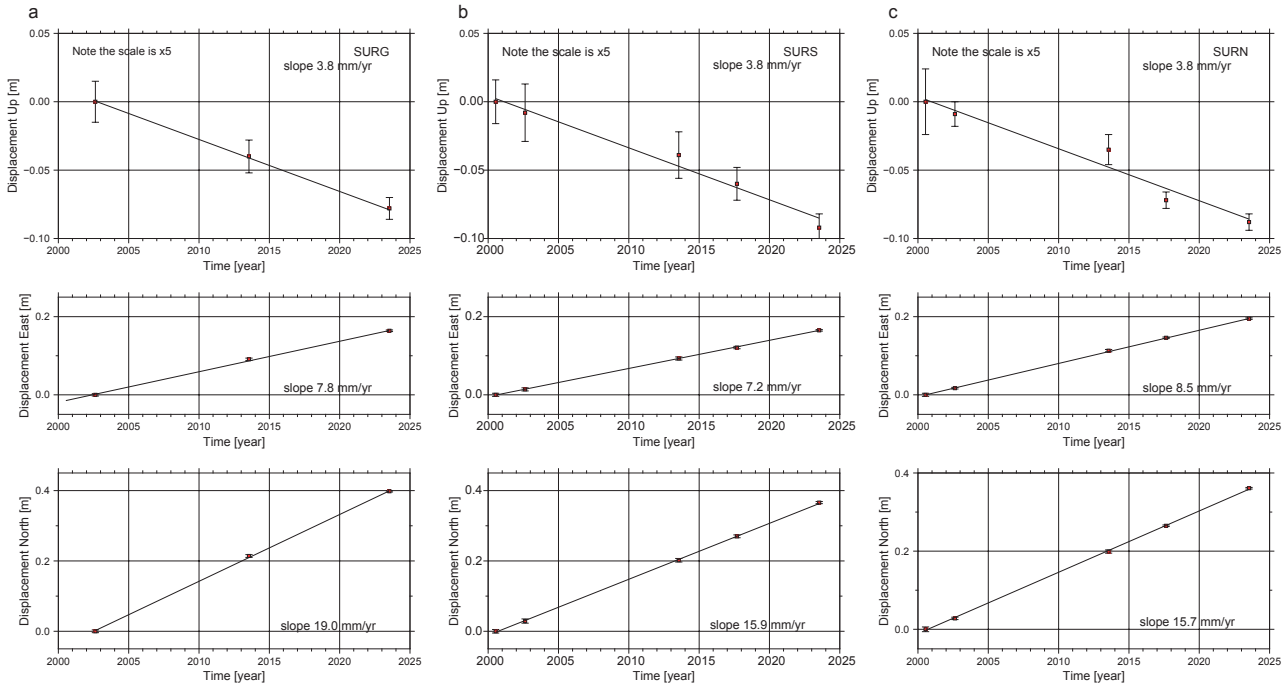

Figure 5. a: Time series for GPS station SURG in the IGS14 reference frame. The vertical displacement appears linear, but with only three points, with a total subsidence of 78 mm since year 2002. b: Time series for GPS station SURS in the IGS14 reference frame (BM 621). The vertical displacement gives a total subsidence of 92 mm since year 2000. c: Time series for GPS station SURN in the IGS14 reference frame. The vertical displacement gives a total subsidence of 88 mm since year 2000.

purpose of a GPS-point in the helicopter platform is mainly for aerial photography as the concrete plate makes an excellent aerial marker. In 2013 and 2023 SURS, SURN and SURG were measured. SURS was also measured in 2017 during drilling operations on Surtsey.

Each GPS point was measured using an antenna on a tripod, collecting data sampled every 15 seconds for approximately 36 to 72 hours. The collected data (2000–2023) were processed using the GAMIT/GLOBK software package (version 10.7, Herring *et al*. 2010). Site positions were determined for each UTC Day in the IGS14 reference frame by referencing over 100 global stations (see Hreinsdóttir *et al*. 2009 for details). The data were corrected for ocean tidal loading effects using the FES2004 model (Lyard *et al*. 2006). For each campaign the average station coordinates and displacements relative to the earliest point in the time series were computed (Table 2). The plate motion model of Altamimi *et al*. (2016) was used to transform the time series from a no-net-rotation reference to stable Eurasia (Table 2). We then calculated the displacement rate from the best fitting line through the data (Figs. 5a–c). The horizontal displacement vectors relative to stable Eurasia (Fig. 6), show similar rates of movement with slight deviation from Eurasia.

Time series for GPS sites SURG (Fig. 5a), SURS (Fig. 5b) and SURN (Fig. 5c), are presented within the IGS14 reference frame. The horizontal displacements are a straight line, indicating constant horizontal velocities. The vertical time series, however, do not fit a straight line as well. Whether the deviations are due to measurement noise or real changes in the subsidence rate is uncertain. The average vertical rates for the three stations are quite similar, with a subsidence of approximately 3.8 mm/yr.

RESULTS

Vertical deformation observations

Overall, Surtsey has been subsiding at a declining rate (Fig. 3). We model the decay as a power law, where D is the vertical displacement, D_0 is chosen such that D-D_0 approaches zero with time, N is the number of years since start of measurements, and p the power law exponent. We find that $p = -0.128$ and $a = 2$ *m* fits the data reasonably well (R^2=0.978). To apply a

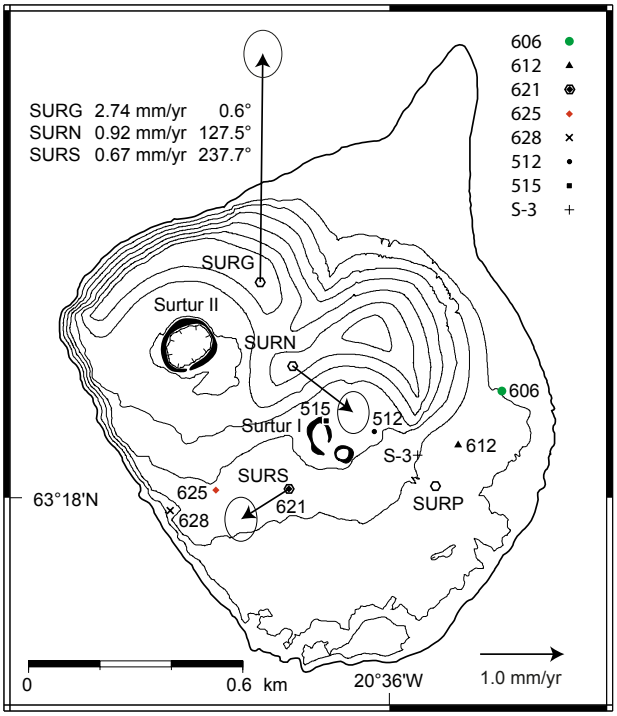

Figure 6. Map of GPS and selected levelling points. The horizontal velocities from GPS measurements 2000–2023 and 2002–2023, relative to Eurasia, are shown as black arrows. Levelling benchmarks are coded by colour and symbol for ease of recognition in subsequent time series figures.

power law equation on negative values is difficult, therefore the data differences are arbitrarily shifted by a constant of 2 m to make all values positive. Subsequently, obtained values are shifted down into the negative range for plotting purposes.

Significant spatial variations are observed in vertical deformation along the levelling line. In all surveys except 1967 and 1991 all benchmarks subsided relative to the water level in WP. The subsidence from August 1967 to August 1991 relative to sea level (WP) was 80–130 cm (Moore *et al*. 1992). During 1967–1968 the subsidence rate was at its maximum at 15–20 cm/year (Tryggvason 1972) and had slowed down to 1–2 cm/year between 1988 and 1991 (Moore *et al*. 1992).

Having been measured in every survey, benchmark (BM) 606 was used as a reference point until 1991 (Moore *et al*. 1992, Sturkell *et al*. 2009).

In recent measurements (1991 onwards) BM 621 was used as the reference for the levelling line and has been surveyed with GPS since 1992. BM 621 has been measured in all surveys but one, as it was not measured 1979 (Table 1a in Sturkell *et al*. 2009). Vertical changes from 1967 to 2023 of selected

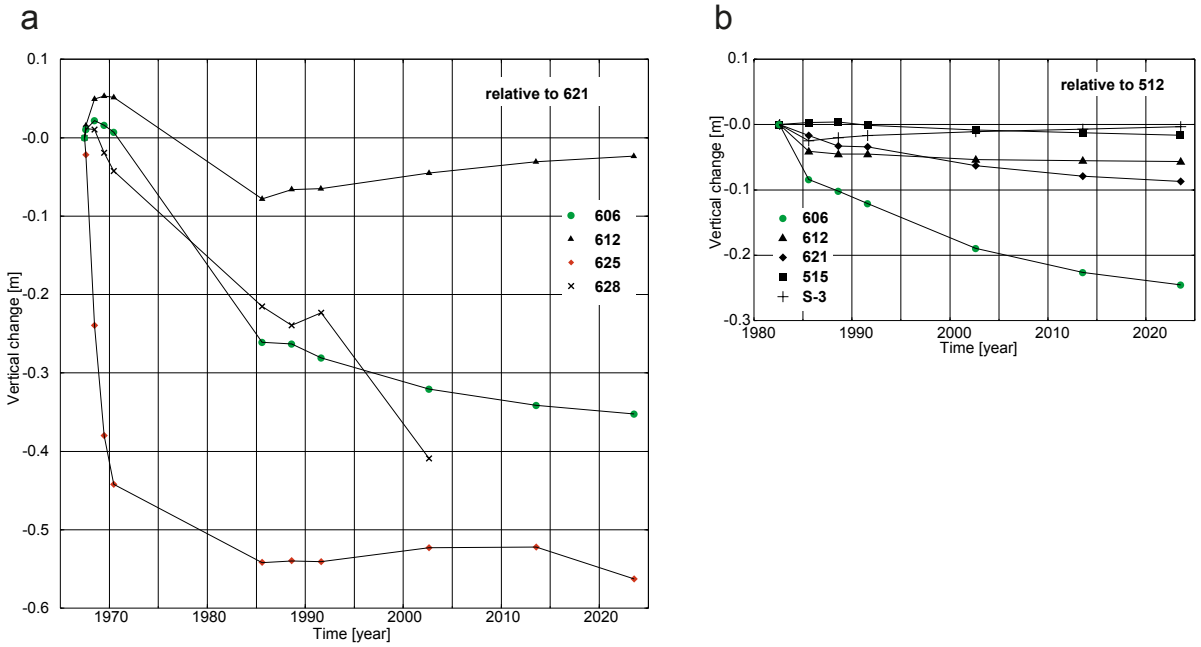

Figure 7. Vertical displacements of selected benchmarks (Fig. 6). The estimated uncertainty of levelling between benchmarks is ±0.1 mm. However, on Surtsey the weather conditions are not always perfect so an estimated uncertainty might be ±0.2 mm. **a:** Displacements relative to BM 621 (the GPS point SURS). Maximum vertical displacements were observed at BM 625 during the first years, slowing down until 1985 and thereafter following BM 621 closely. Currently BM 606 shows the most rapid subsidence if BM 628 is excluded. **b:** Vertical displacements of selected benchmarks (Fig. 6) since 1982 relative to BM 512. BM 515 and BM S-3 have the smallest vertical displacements. They are located on a thin lava flow that overlies the Surtur 1 tuff cone. Benchmark 606 near the eastern coast, used as a reference by Moore *et al*. (1992), has the highest subsidence rate relative to BM 512 in this group of benchmarks. Note, currently BM 606 has the highest rate relative to BM 621.

Table 2. GPS displacements for sites SURS, SURN and SURG. The displacements are in the IGS14 reference frame and relative to the earliest data point.

SURS

Year	N [m] IGS14	N [m] Eurasia	Uncertainty	E [m] IGS14	E [m] Eurasia	Uncertainty	Up [m]	Uncertainty
2000.531	0	0	0.0047	0	0	0.0032	0	0.0153
2000.534	0.0015	0.0015	0.0039	0.0002	0.0002	0.003	-0.0036	0.0125
2000.537	0	-0.0001	0.0067	-0.0034	-0.0034	0.0047	-0.0050	0.0206
2002.623	0.0305	-0.0035	0.0087	0.0127	-0.0036	0.0055	-0.0026	0.0347
2002.626	0.0305	-0.0036	0.0027	0.0138	-0.0025	0.0020	-0.0122	0.0087
2002.629	0.0283	-0.0058	0.0057	0.0122	-0.0041	0.0043	-0.0165	0.0192
2013.547	0.1960	-0.0156	0.0072	0.0935	-0.0076	0.0046	-0.0440	0.0199
2013.549	0.2090	-0.0027	0.0049	0.0896	-0.0115	0.0038	-0.0352	0.0149
2013.552	0.2021	-0.0096	0.0043	0.0924	-0.0088	0.0032	-0.0419	0.0128
2013.555	0.2033	-0.0085	0.0056	0.0913	-0.0099	0.0046	-0.0448	0.0194
2017.689	0.2710	-0.0080	0.0035	0.1207	-0.0126	0.0023	-0.0680	0.0114
2017.692	0.2697	-0.0093	0.0043	0.1194	-0.0139	0.0034	-0.0580	0.0130
2023.533	0.3652	-0.0088	0.0038	0.1628	-0.0159	0.0028	-0.0921	0.0123
2023.536	0.3669	-0.0072	0.0028	0.1649	-0.0138	0.0023	-0.0933	0.0084
2023.538	0.3676	-0.0065	0.0028	0.165	-0.0138	0.0023	-0.0980	0.0087

SURN

Year	N [m] IGS14	N [m] Eurasia	Uncertainty	E [m] IGS14	E [m] Eurasia	Uncertainty	Up [m]	Uncertainty
2000.537	0	0	0.0093	0	0	0.0058	0	0.0371
2000.54	0.0009	0.0009	0.0032	0.0034	0.0034	0.0023	-0.0075	0.01
2002.623	0.0295	-0.0044	0.0024	0.0186	0.0024	0.0017	-0.0102	0.0076
2002.626	0.0292	-0.0048	0.0020	0.0191	0.0029	0.0016	-0.0117	0.0065
2002.629	0.0279	-0.0061	0.0033	0.0193	0.0030	0.0026	-0.0158	0.0115
2013.547	0.1952	-0.0163	0.0039	0.1169	0.0158	0.0026	-0.0537	0.0109
2013.549	0.2064	-0.0052	0.0041	0.1124	0.0113	0.0033	-0.0393	0.0123
2013.552	0.2004	-0.0112	0.0032	0.1153	0.0142	0.0025	-0.0524	0.0094
2013.555	0.1977	-0.0140	0.0037	0.1128	0.0117	0.0039	-0.0454	0.0128
2017.640	0.2656	-0.0125	0.0022	0.1472	0.0143	0.0015	-0.0783	0.0070
2017.642	0.2658	-0.0123	0.0021	0.1467	0.0138	0.0016	-0.0747	0.0063
2017.645	0.2663	-0.0119	0.0018	0.1483	0.0154	0.0015	-0.0731	0.0055
2023.536	0.3609	-0.0131	0.0022	0.1965	0.0178	0.0017	-0.0896	0.0068
2023.538	0.3615	-0.0125	0.0017	0.196	0.0173	0.0015	-0.0949	0.0053

SURG

Year	N [m] IGS14	N [m] Eurasia	Uncertainty	E [m] IGS14	E [m] Eurasia	Uncertainty	Up [m]	Uncertainty
2002.629	0	0	0.0038	0	0	0.0027	0	0.0130
2002.632	-0.0012	-0.0012	0.0046	0.0007	0.0007	0.0035	-0.0138	0.0172
2013.547	0.2076	0.0301	0.0044	0.0938	0.0090	0.0029	-0.0504	0.0124
2013.549	0.2191	0.0415	0.0044	0.0889	0.0041	0.0035	-0.0372	0.0134
2013.552	0.2133	0.0357	0.0034	0.0914	0.0065	0.0026	-0.0504	0.0102
2013.555	0.2127	0.0350	0.0038	0.0894	0.0045	0.0039	-0.0492	0.0132
2023.536	0.3967	0.0568	0.0027	0.1642	0.0018	0.0020	-0.0814	0.0088
2023.538	0.3971	0.0571	0.0021	0.1638	0.0013	0.0018	-0.0893	0.0064

benchmarks (Fig. 6) relative to BM 621 are presented in Figure 7. BM 606 appeared to have a constant rate during the first few years but then plunges into subsidence. BM 612 rose in the first years relative to BM 621, subsided until 1985 and has been rising since. BM 628 subsided 0.4 m until it was lost to the sea, sometime between 2002 and 2013. The cliff hosting BM 627 was lost to sea sometime between 2013 and 2023. The 2003 survey shows accelerated subsidence at BM628, most readily interpreted as the benchmark cliff edge had already started giving in to the sea.

Based on the levelling data we can infer which parts of the island are most stable. From the 1985 survey onwards the relative displacement between BM 606, near the eastern shore, and BM 625 (Fig. 7a), near the southwestern shore, is relative stable. In the period 1985 to 2013 the BM621 had very limited vertical displacement. In the most recent survey BM625 has started to subside. This is likely because of its growing proximity to the southwestern coastline. The steep cliff to the southwest of the island is currently affected the most by intense erosion (Óskarsson *et al.* 2020). These authors also report a system of cracks running parallel to the cliff, about 1–5 meters into the lava field with cracks that can be up to 170 meters long.

Benchmarks 512 to 520 showed about 8 cm of uplift relative to BM 606 in the period 1982–1985 decreasing to 2 cm in the period 1985–1988 (Moore *et al*. 1992). This indicates that the most "stable" area (i.e., with the least subsidence) is around BM 512, in vicinity of the Surtur 1 crater near the centre of the island (Fig. 6). After 1985, benchmarks 612, 621, S-3, and 515 kept rather stable relative to BM 512, while BM 606, near the NE coast started a steady subsidence **(**Fig 7b). Overall, the benchmarks closer to the sea subside faster compared to the benchmarks in the inner parts, especially around Surtur I.

With GPS measurements from 1991, an absolute elevation-reference could be established for the levelling line instead of relying on water level measurements in the dug pit. The GPS measurements also add information of horizontal deformation. The GPS site SURS (BM 621) subsided 8 ±1 cm between 1992 and 2000 relative to sites REYK and ARNA in Reykjavík (Sturkell *et al*. 2009), giving an average rate of 10 mm/yr. The absolute subsidence of SURS between 2000 and 2023 is 9.2 cm (Table 2), corresponding to a subsidence rate of 3.8 mm/yr (Table 3).

Table 3. Velocities of GPS stations in the IGS14 and Eurasian reference frames. Units are in mm/yr unless otherwise noted.

Station Reference	N	E	U	Horizontal rate	Azimuth [°]
SURS IGS14	19.0	7.8	-3.8	20.5	24.9
SURG IGS14	15.9	7.2	-3.8	17.4	27.9
SURN IGS14	15.7	8.5	-3.8	17.8	34.5
SURS Eurasia	2.7	0.0	-3.8	2.7	0.6
SURG Eurasia	-0.4	-0.6	-3.8	0.7	237.7
SURN Eurasia	-0.6	0.7	-3.8	0.9	127.5

The 1993 and 2004 nationwide ISNET GPS campaigns (Árnadóttir *et al*. 2009) are useful to estimate the regional deformation field that may affect our estimate of the subsidence of Surtsey. Using the ITRF2005 (Altamimi *et al*. 2007) reference frame, Árnadóttir *et al*. (2009) obtained a subsidence of 0.4 ± 0.8 mm/yr and uplift of 3.2 ± 1.5 mm/yr for sites 0082 (Valhúsahæð, Reykjavík) and 0353 (Heimaey), respectively, resulting in a net uplift rate of 3.6 mm/yr of Heimaey relative to Reykjavík. This result is similar to the rate of 3.5 ± 1.5 mm/yr of site VMEY relative to REYK estimated by Geirsson *et al*. (2006), using continuous GPS data from 2000 to 2004. It has been established that a large part of Iceland is rising because of glacial isostatic adjustment (GIA, Árnadóttir *et al*. 2009, Cao *et al*. 2023). The glacial rebound model of Árnadóttir *et al*. (2009) predicts a differential uplift of VMEY (and site 0353) relative to REYK (and 0082) of 1.5 mm/yr. This difference will be slightly smaller for Surtsey since it is at a greater distance from the ice caps than Heimaey, perhaps 1 mm/yr. Considering the average subsidence rate of BM 621 during 1992 to 2002 (~1 cm/yr), we thus regard the glacio-isostatic effects as of little importance for this time period. However, GIA in Iceland has accelerated due to warming climate (Geirsson *et al*. 2012, Cao *et al*. 2023), so the recent (~20 years) deceleration in subsidence at Surtsey may be partly explained by faster regional uplift due to GIA. In fact, assuming ~2–3 mm/yr increase in GIA since after 2004 (as suggested by Geirsson *et al*., 2012), nearly half of the subsidence decrease from ~1 mm/yr in 1992–2002 to 3.8 mm/yr in 2002–2023 may be explained by faster GIA. More detailed GIA models are being developed that will be of importance to quantify this effect better (Bellagamba *et al*. 2024).

Table 4. Combination of GPS data at SURS (BM 621) with the levelling results between the WP and BM 621.
A: The height changes relative to the water pipe (WP) site and the BM 621 between June 1967 to 1991.
B: The cumulative subsidence from the GPS measurements 2000–2023 (Table 2) relative to year 2000.
C: The combined vertical displacements for BM 621 (see also Figure 2).

A.

Year	WP to 621 [m]	displacement [m]
1967 June	511409	0
1967 Aug	512333	0.0924
1968	51175	0.0341
1969	508494	-0.2915
1970	507541	-0.3868
1982	50497	-0.6439
1985	50413	-0.7279
1988	50306	-0.8349
1991	50391	-0.7499

B.

Year	displacement [m]
2000	0.0000
2002	-0.0076
2013	-0.0386
2017	-0.0601
2023	-0.0916

C.

Year	displacement [m]
1967.5	0
1967.7	0.0924
1968	0.0341
1969	-0.2915
1970	-0.3868
1982	-0.6439
1985	-0.7279
1988	-0.8349
1991	-0.7499
1992	-0.7599
2000	-0.8699
2002	-0.8779
2013	-0.9089
2017	-0.9299
2023	-0.9619

Using the levelling data from 1967 to 1991 and the GPS data of 1992–2023 to constrain elevation changes of BM 621 relative to WP (Fig. 6, Table 4), we obtained the absolute vertical displacement of BM 621. The GPS subsidence rates observed 1992–2002 were applied to the one-year gap 1991–1992. The absolute vertical data is dominated by subsidence. The only interval that shows uplift is between the first two measurements in 1967. The data (Fig. 4) shows higher subsidence rates during the first ten years and lower subsidence rates from 1982 onwards.

Models of Vertical Deformation

At least seven geological processes possibly contribute to the vertical displacement of Surtsey (e.g., Moore *et al*. 1992):

a) lithostatic load from the weight of the erupted material, b) compaction of the pre-existing seabed sediments (vertical strain), c) palagonitization of the tephra, d) compaction of the volcanogenic material, e) thermal contraction of the lava field; and f) magma withdrawal or other movements in the magmatic plumbing system. We do not consider thermal contraction of the tuff under the lava flows as they were cooled by seawater directly as they formed. We discuss each of the processes mentioned above in the following sections.

Lithosphere flexure

To calculate the load effect caused by the added weight of Surtsey on the lithosphere we assume a surface load that will cause time-dependent flexure of the lithosphere. We implement a model detailed in Islam (2016). The shape of Surtsey is nearly circular and simplified to a cone (Fig. 8a). The width of Surtsey is estimated to be 3200 m along a profile which crosses the centre of Surtsey aligned N125°E. The two small temporal islands Jólnir and Syrtlingur were not included in the model. The total elevation of the Surtsey edifice is 260 m with half under water (Fig. 8a). The load is calculated using radial symmetry in three segments; AB = 400 m, BC = 400 m and CD = 800 m (Fig. 8b) and $P = \rho gh$ where ρ represents the density of Surtsey, assumed to be 1800 kg/m^3, g is gravitational acceleration and h is height. For the submarine part of Surtsey, the buoyancy effect is managed by considering density difference (Δρ) between seawater and Surtsey. The load on segment AB is calculated as

P_{AB} = Δρg×130m + ρg×65m + ρg(0.5×65m) =

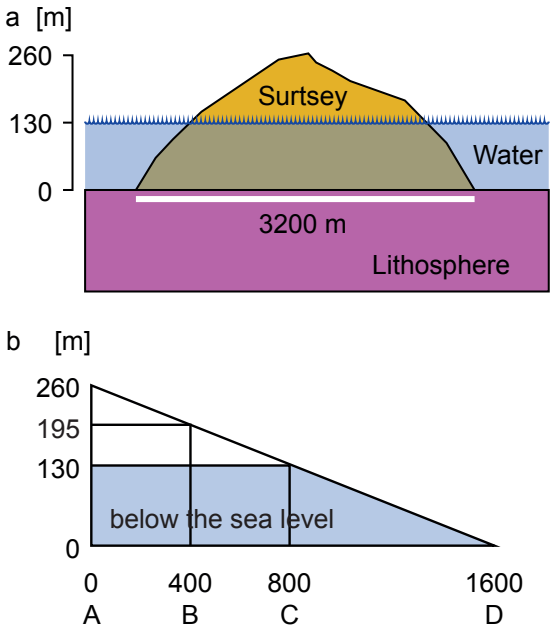

Figure 8. Modelling Surtsey. (a) Surtsey is simplified as a cone with its lower half below sea level. (b) Axisymmetric shape of one-half of Surtsey for calculation of its circular load. Here A designates the centre of Surtsey. The load is distributed along the radius profile in three segments. e.g., AB, BC, and CD.

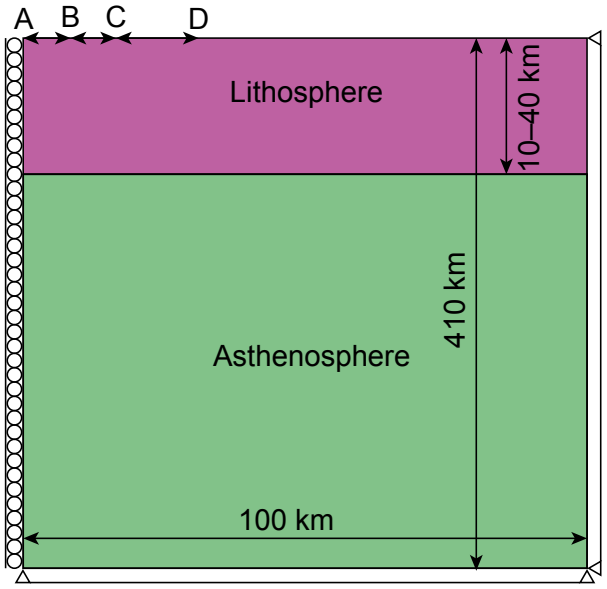

Figure 9. Geometry and boundary conditions of two-dimensional circular-load models. "A" designates the centre of Surtsey. We apply roller conditions on the left axis, allowing this vertical section to move only vertically, and being fixed horizontally. The bottom and vertical right boundaries are fixed. The length of AD is the radius of Surtsey. The length of AB, BC and CD is as in Figure 7b, however, shown here in exaggerated scale compared to the model dimensions. Different lithospheric thicknesses and viscosities were tested.

800kg/m^3×9.82m/s^2×130m + 1800kg/m^3×9.82m/s^2×65m + 1800kg/m^3×9.82m/s^2×(0.5×65m) = 2.7 MPa. The load for segments BC and CD is similarly calculated as 1.6 and 0.5 MPa, respectively.

The loading calculations of Surtsey on the lithosphere as well as on the asthenosphere is conducted by two-dimensional circle-load axisymmetric mechanical models using commercial Finite Element Modelling package Abaqus/CAE 6.11. The width and depth of the model space is 100 × 410 km, respectively (Fig. 9). The depth of the model is constrained by the depth of lithosphere and asthenosphere. The width is kept ~60 times larger than the length of applied load to avoid boundary effects.

Our model has two uniform layers: a viscoelastic asthenosphere beneath an elastic lithosphere. Different lithospheric thicknesses (30 to 65 km) were tested using three different Newtonian viscosities of the underlying asthenosphere (Figs. 9 and 10). The models ran for a period set to 50 years by applying the instantaneous load calculated in the previous section. The Winkler Foundation is given by $\Delta\rho g$ where ρ is density and g is the gravitational acceleration as Archimedes' principle of boundary condition to maintain isostasy (see Wu (1992) for

Table 5. Mechanical material properties of the loading model. The density of Surtsey is based on Moore *et al.* (1992), and properties of the lithosphere and asthenosphere on Turcotte & Schubert (2002:436). The viscosity of the asthenosphere beneath Surtsey is assumed as similar as beneath Iceland from glacioisostatic studies (Auriac *et al.* 2013; Barnhoorn *et al.* 2011; Pagli *et al.* 2007).

Parameters		Value
Surtsey	Density, ρ_S (kg m^{-3})	1800
Seawater	Density, ρ_w (kg m^{-3})	1000
Lithosphere	Average density, ρ_L (kg m^{-3})	2950
	Young's modulus, E_L (Pa)	8×10^{10}
	Poisson's ratio, ν_L	0.25
Asthenosphere	Average density, ρ_A (kg m^{-3})	3350
	Young's modulus, E_A (Pa)	1.3×10^{11}
	Poisson's ratio, ν_A	0.28
	Viscosity, η (Pa S)	3×10^{18}, 5×10^{18}, 1×10^{19}
Gravitational acceleration, g (m S^{-2})		9.82

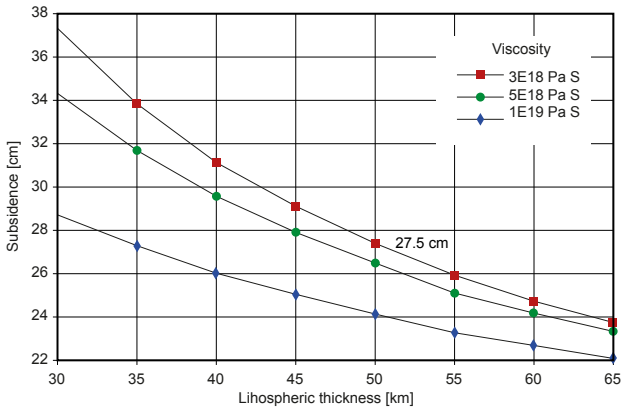

Figure 10. Three circular-load models of Surtsey, spanning 50 years. Total subsidence at the centre of the model, calculated for different asthenosphere viscosities.

more details). Winkler Foundation was applied at the surface (where Δρ is density difference between water and lithosphere) and at the interface between the lithosphere and asthenosphere (where Δρ is density difference between lithosphere and asthenosphere). Other boundary conditions are described in Figure 9. The mechanical properties used in our modelling are presented in Table 5.

The strain models contain three-node linear triangle elements. Deformation is calculated as sum of elastic and creep responses (see Wu (1992) for more details). Abaqus (2011, pages 21.2.1-1 and 22.2.4-4) derives elastic response using Hooke's principle, where the total stress $\sigma = C^{el}\varepsilon^{el}$ where C^{el} is the fourth-order elasticity tensor and ε^{el} is the total elastic strain. Creep response is conducted by a power law for the strain rate: $\delta\varepsilon = [A\sigma^n\{(m+1)\varepsilon\}^m]^{1/(m+1)}$, where A is a material parameter, n is the power of the stress σ, and m is the power of the strain hardening. The Newtonian viscosity can be related to this power law by inserting m=0 and A=1/(3η), if normal stress and strain rate are considered (Ranalli 1987, p. 75–80).

Loading models (Fig. 10) for different viscosities (3, 5, 10 x 10^{18} Pa s), and lithospheric thicknesses ranging from 30-65 km yield a total subsidence ranging from 22 to 37 cm, or approximately 1/3 of the currently observed subsidence. The subsidence over 50 years for a 50 km thick lithosphere and a viscosity of 3×10^{18} Pa s is 27.5 cm. Thinner lithospheric plates and lower viscosities predict higher subsidence. Surtsey is located on the edge of the Icelandic mantle plume. Considering the inferred lithospheric thickness of ~50 km and the intermediate thermal regime beneath Surtsey, an average asthenospheric viscosity of approximately 3×10^{18} í Pa s provides the best fit for the study area. The lithosphere is getting thinner towards the south into normal ocean crust thickness. The viscosity is probably in the lower end.

Palagonitization and consolidation

The degree of alteration of the original basaltic tephra is related to the temperature of the hydrothermal fluid (Jakobsson 1978, Jakobsson & Moore 1986). At temperatures of 100 °C, the main constituent of the tephra, the sideromelane glass, turns into palagonite, and consequently, the rock is consolidated. Jakobsson (1978) estimated that already in 1975, 64% of the two tephra-cones in Surtsey had consolidated to dense palagonite tuff. The porosity of the basaltic tephra in Surtsey is reduced in the palagonitization process as pores become filled with secondary minerals, thus causing net contraction of the hyaloclastite as pores are filled partly by the rocks' own materials. Assuming this effect could cause 1 % reduction pore space could cause as much as 2 m of subsidence. However, as pore space is also decreased by compaction (Section 5.3) it is difficult to separate these two mechanisms.

Compaction of pre-existing sea-bed sediments

The new island was built up on top of sediments, and the added weight will cause some compaction of the unconsolidated seabed deposits. To evaluate this contribution, the total amount of unconsolidated sediments must be estimated. In 1980 two seismic reflection profiles were measured just south of Surtsey across the submarine part of Jólnir (Thors & Jakobsson, 1982). The profiles show volcanic features resting on a stratified sequence with layering visible some 100 meters below the seafloor. Thors & Jakobsson (1982) interpreted a reflector as the top of Pleistocene. We assume this reflector marks the bottom of the unconsolidated sediments and evaluate the thickness of the Holocene deposit from the reflector up to the seafloor, using the east-west profile located 1–2 km south of Surtsey. The two-way travel time to the reflector is 17 ms. Thus, assuming a compressional velocity for the seafloor sediments of 1650 m/s gives thickness of the Holocene sediments as approximately 14 m. However, the reflector undulates so values of 14–20 m for unconsolidated sediments at the Surtsey eruptive site are reasonable.

We assume the porosity – depth relation is exponential and use sea bottom porosity of f_0 = 49% and a porosity-depth coefficient c = 0.27 km^{-1} for

sandstone (Sclater & Christie (1980: page 3732)). The relation $f = f_0 e^{-cy}$ gives the porosity at depth y, which decreases from the initial porosity because of the weight of the overload. Using a load corresponding to 130 m (Fig. 8) applying the formula ($f_0 - (f_0 e^{-cy})$) for porosity change gives 0.49 – (0.49e-0.27*0.13) = 0.017, or a porosity reduction of 1.7 %, which for the 20 m thick sediments gives a compaction of 34 cm. At the vent we presume unconsolidated sediments were blown out by the eruption.

Compaction of volcanoclastic materials

The tuff and hyaloclastite (breccia and coarse to fine-grained sandstone) are subject to gravity-driven compaction. Porosity decreases as the compaction and cementation increase with time. The material will compact from its own weight and applying the calculations above for the seabed sediments gives an average porosity loss of 1.7 % "(at the top zero compaction and at the base 1.7 % compaction) gives 1.7/2 = 0.85 % and with 130 m of material the resulting subsidence will be 110 cm.

Thermal contraction

Fresh lava flows will exhibit subsidence due to thermal contraction. This subsidence acts in proportion to the thickness of the lava and it decays with time. At Etna, Sicily, for example, lava flows show a subsidence rate of 0.7 mm/day (256 mm/yr) during the first 70 days of a 50-m thick lava. The subsidence rates then decay rapidly (Stevens *et al*. 2001). It is suggested that lava flows of Etna that are thicker than 30 m can continue to subside for up to 20 years (Stevens *et al*. 2001). The lava flows at Surtsey are of similar thickness and they are intercalated by numerous scoria horizons. Early on. thermal contraction was probably a sizable contributor to the subsidence at Surtsey.

Measurement of tidally driven rise and fall of hot water within the drill hole demonstrates the importance of water circulation within the volcanic pile. This no doubt sped up thermal contraction during the first years. The thermal contraction during the first 20 years was larger than in recent years so that current subsidence is probably little affected, compared to Etna.

Thermal logging repeated in the borehole (Perez *et al*., 2022) shows mainly two areas of cooling: above sea-level (cooling of up to 60°C during 1980–2018) and a narrow area approximately 50 m below sea-level (cooling of up to 20°C during 1980–2018). Weaver *et al*. (2020) experimentally found a value of 5 x 10^{-6} /°C for the thermal expansion coefficient for hyaloclastite sampled at 70 m depth in Krafla, comparable to typical values for basalts and glass (0.5-9 x 10^{-6} /°C). We can use these values to find a range of possible effects of thermal contraction on subsidence, assuming thickness of 200 m. We do not know the thermal evolution prior to 1980; however, it is likely the maximum temperatures were on average below the boiling curve (maximum 160°C) since the tuff is deposited into cool ocean waters. Assuming an average minimum (maximum) temperature change of 10°C (100°C) and a minimum (maximum) thermal expansion coefficient of 0.5 x 10^{-6} /°C (5 x 10^{-6} /°C) we obtain possible total subsidence of 1 mm to 10 cm for contribution of thermal contraction.

Magma withdrawal or other movements in the magmatic plumbing system

A study of U-series disequilibria in the volcanic products of Surtsey indicates that they originated in the mantle and rose to the surface on a timescale shorter than a decade (Sigmarsson 2013). No indications support the existence of a shallow-level storage region. Because surface deformation for deep sources is small, the magmatic system likely has negligible effects. Furthermore, one might rather expect inflation and uplift following the eruptions, as in Krafla (e.g., Tryggvason 1994).

Land erosion of Surtsey

Óskarsson *et al*. (2020) identify three main processes related to the erosion of Surtsey; 1) A rapid initial erosion, 2) the prevailing SW coastal wave erosion, and 3) intense wind and runoff erosion. In the beginning a rapid erosion of the lava apron by wave erosion took place. Additionally, the unconsolidated tephra suffered by erosion. After the initial erosion slowed down (during 1967–1974) and became minor, the prevailing wave action from the southwest was still very efficient. According to figure 6 in Óskarsson *et al*. (2020) the southwest flank of the island lost 9.7 million m^3 from 1967–74 (1.38 million m^3 /year) and 18.4 million m^3 from 1974–2019 (0.41 million m^3 / year). This is a drastic drop in Surtsey's erosion rate but with time it adds up to considerable volumes. Eysteinn Tryggvason installed a levelling line across the island with twelve of the benchmarks up to number 624 along the southwest coast of Surtsey (Tryggvason 1968). In 1985 the end of the line

was marked by benchmark 633. In the most recent survey benchmark 626 represented the end of the line. Óskarsson *et al*. (2020) also address the wind redeposition of sand. This drifting sand has hidden several benchmarks but also exposed some. Since the end of the eruption in 1967 to 2019 over 53% of Surtsey's area has been lost, however, with the erosion rate decreasing with time (Óskarsson *et al*. 2020).

DISCUSSION

Deformation observations

Subsidence has been observed at Surtsey from 1967 through 2023 relative to an external reference frame; first the tidal pond and since 1992 by GPS in relative or absolute terms (Fig. 4). A subsidence rate of 10 mm/yr (1992–2002), and 3.8 mm/yr (2000–2023) is observed for BM 621.

The most "stable" benchmarks are BM 512 and S-3 (Fig. 6), as they subside the least (Table 1). The relative uplift rates 1991-2023 for BM 512 and S-3 relative to BM 621 are 1.7 mm/yr and 2.1 mm/yr, respectively. In the period 1991 to 2002 the BM 512 was the most "stable" and in the two most recent measurements (2017-2023) the S-3 is the most "stable". All the benchmarks close to the Surtur-I crater have uplift relative BM 621. We note that no measurements have been done around the crater Surtur-II (Fig. 2). The least stable (i.e., fastest subsiding) benchmarks are at the edge of the island, and indeed many have been lost to sea already due to erosion. The accelerated subsidence observed prior to when the benchmarks are lost is due to slope failure processes, as the rocks have begun detaching and sagging before failing completely (e.g., Leshchinsky *et al*. 2019).

The horizontal motion of GPS sites largely follows the Eurasian plate (Fig. 6). Deviations of a few mm per year need though to be explained. There are variations in the vertical deformation across the island (e.g., Fig. 7), which likely also have horizontal counterparts.

Comparison of subsidence processes

The different processes considered here to affect vertical deformation of Surtsey are: 1. the lithostatic load of the erupted material; 2. compaction of seabed sediments; 3. palagonitization of the tephra; 4. compaction of the volcanogenic material; 5. thermal contraction of the lava field; and 6. the magmatic plumbing system. These have different spatial behaviour and temporal spans. Some decay rapidly, some slower. The different subsidence processes generate different amounts of subsidence, ranging from essentially zero to meter-level displacements. Compaction of the volcanoclastic pile predicts the largest displacements of our models. Each of our models relies on various assumptions, often leading to uncertain values.

The finite element load model (Section 5.1) predicts up to 27.5 cm of subsidence in the first 50 years (Fig. 10). The centre of the Icelandic mantle plume is in the north-western part of Vatnajökull, situated approximately under Bardarbunga (Fig. 1). Surtsey is located at 150–200 km's distance from the central part of the mantle plume. With Surtsey far from the mantle plume centre, and into "normal" ocean crust suggests effectively thinner lithosphere and lower viscosity, such that total subsidence due to loading may be more reasonable at 25-30 cm since the formation of Surtsey. The asthenosphere response to the load is still ongoing, with a rate today less than 3.8 mm/yr. The load model would give an exponential subsidence of the island. The amount of subsidence of the GPS site SURS (BM 621) since year 2000 is 91.6 mm or 3.8 mm/yr. During the same time interval, the relative subsidence between S-3 and BM 621 is 67 mm (Fig. 7b, Table 3). The S-3 and BM 512 (Fig. 6) are close to the feeder conduit and this is expected to be the most "stabile" area as the tephra is almost completely palagonitized. The compaction of sediment and volcaniclastic rocks (Sections 5.2-5.4) contributes very little today.

We therefore suggest that all vertical deformation of the benchmarks (512 – 518 and S-3 & 4) in and around the Surtur I crater, that have moved uniformly, are to the greatest extent caused by the lithospheric load. The subsidence from the lithospheric load is today 1.1 mm/yr.

The erosion and sedimentation described by Óskarsson *et al*. (2020) gives a picture of the dynamics of the surface of the island. In the period 1974–2019 the dDEM reveal massive erosion to the southwest and the south there the lava apron is lost to the sea. Also, the north-western rock face of the Surtur II (Surtungur) experienced significant erosion. The shifting sand on the island accumulates primarily on the northern and eastern flank of the eastern tuff cone (Surtur I). The amount of sedimentation

suggested in figure 3 in Óskarsson *et al*. (2020) is up to 6.5 m and erosion of the eastern tuff cone is at one place 22.8 m. However, these are small areas that show these numbers and this has no effect on the lithospheric load. All the benchmarks are in bedrock, and some are buried under sediments or eroded away on the southwest flank of the island.

In the most recent survey 2023, the end of the levelling line is at benchmark 626 which has started to subside faster. In the period 2013–23 it subsided 4.0 cm (with BM 621 fixed). The cliff is moving outward to the sea and after a short time this benchmark will be gone. Benchmark 625 is getting closer to the cliff face and it is moving outward. The open cracks described by Óskarsson *et al*. (2020) are growing and one runs between benchmarks 625 and 626.

The time series of the vertical displacement relative to BM 621 (Fig. 7a) indicate high subsidence rates during the first twenty years since the island formed (until 1985). This pattern is also observed relative to BM 512 (Fig. 7b). Since 1985, two sites close to BM 512 (BM 515 and BM S-3) experienced only small changes, and the two benchmarks 612 and 621 have a low relative subsidence rate (Fig. 7a). This excessive subsidence is probably caused by compaction of loose volcanogenic and seabed material. The closer to the crater and the feeder dykes the more stable the ground gets. Closer to the shoreline (the lava feed delta) and away from the crater the material is less compacted. Also, the seaside offers less support than the land side. The suggested compaction seems to decline with time and is today less than 1 mm/yr.

In 1979 a 181 m deep hole was drilled on Surtsey ending just a few meters above the original seabed (SDH-1 in Fig. 2). The final meters of the drilling penetrated loose tephra (Moore *et al*. 1992), which indicates that the palagonitization reaches almost down to the original seabed at the drill site. Three drill holes were made in 2017 at almost the same location (SE02a-b, SE03 in Fig. 2): two vertical holes (combined length 186 m) and the third 354 m long, dipping 55° in direction 264°W toward the Surtur-I crater (Moore & Jackson 2020). Over 95% of the drill core from 2017 consists of lapilli tuff (McPhie *et al*. 2020). The slanting SE03 drill hole reached a thick (342 to 352 m) coherent basalt just above the end of the drilling, interpreted as the feeder dyke (McPhie *et al*. 2020).

The information from the drilling gives a suggestion of the extent of the palagonitization. Each of the two tuff cones I and II form inverted cones of more or less palagonitized material. As the cones do not overlap completely, an un-palagonitized tuff area is suggested to be present in the core of the island. The GPS site SURN measured in 2000, 2002, 2013 and 2023 is located on the crest that divides the Surtur I and II craters. The GPS measurements of the three sites show a similar subsidence rate (3.8 mm/yr) and they are similar distance from the centre of respective crater (Fig. 8). This indicates a similar amount of palagonitization has occurred under all three GPS sites.

The thermal contraction of the lava flows is comparable to the lava flows at Etna. The contraction was largest in the first 20 years and is now likely negligible. Continued cooling of the hyaloclastite mass, averaged over the length of the borehole, is approximately 0.2°C/yr (Perez *et al*. 2022), resulting in current subsidence rate of 0.2 mm/yr.

The additional subsidence is attributed to compaction of the tuff cone and material in the lava feed delta, with exception of the areas closest to the coast. The deformation of the benchmarks located in the central part of the island is used to estimate the vertical strain caused by the compaction of the tuff and the fragmented (diamictite) material in the lava fed delta. Under the GPS site SURS (benchmark 621) a slightly higher amount of subsidence is observed. Possibly it is located over an area that is less palagonitized.

Need for continued measurements

The vertical strain (subsidence) is currently reasonably small, below 5 mm/yr, but still significant. Both the compaction and asthenosphere response are almost complete for the island. The "major" deformation now and in the future will be that the sides slump out into the sea as the sea erosion digs in. Some of this slumping would be interesting to observe with GPS to capture horizontal motion. The levelling benchmarks were measured kinematically with GPS in 1992 (Einarsson *et al.* 1994), and it may be of interest to add GPS measurements to the levelling observations. There are still subtle changes in deformation across the island that will be interesting to research further with precision levelling every 10 years or so. It may be feasible to apply high-precision modes of InSAR, however, the island is so small, with high topography and abundant sand-drifts, that it would be challenging to detect its slow deformation using that technique.

However, the sagging of sizable blocks by the island edges may well be recorded with repeat precision photogrammetry. Finally, by all chances, another eruption will occur in the Surtsey and Vestmannaeyjar region. It is impossible to say what it's precursors will be, but recent unrest periods in Krafla and Reykjanes Peninsula indicate that detailed seismic and geodetic observations are primary monitoring tools for such precursors. Therefore, geodetic monitoring of Surtsey needs to be continued.

Conclusions

Two processes dominate the subsidence at Surtsey: Flexure of the lithosphere under the load of the new island and compaction of the volcanic edifice. Since the formation of Surtsey with its volume of 0.8 km^3, the load has depressed the surface by 25-30 cm.

ACKNOWLEDGEMENTS.

We are thankful for the transportation support of the Icelandic Coast Guard and the hospitality of the Surtsey Research Society on Surtsey. The authors would like to express their appreciation for all the help from Sveinn P. Jakobsson at the Icelandic Institute of Natural History. During the survey of 2013 we received valuable assistance from Hallgrímur Jónasson and Þórdís Vilhelmína Bragadóttir, and in 2023 from Valdimar Kristjánsson. This text is partly based on an unpublished manuscript in Tariqul Islam's Ph.D. thesis from 2016. Editorial comments from Gabrielle Stockmann improved the manuscript considerably. Comments from an anonymous reviewer have helped us to significantly improve the paper.

REFERENCES

Abaqus, 2011. Analysis User's Manual. Version 6.11. 3. part V. Dassault Syst. Simulia Corp., Providence. USA

Altamimi, Z., X. Collilieux, J. Legrand, B. Garayt, & C. Boucher, 2007. ITRF2005: A new release of the International Terrestrial Reference Frame based on time series of station positions and Earth Orientation Parameters. J. Geophys. Res. 112. B09401. doi:10.1029/2007JB004949

Altamimi, Z., P. Rebischung, L. Métivier, & X. Collilieux, 2016. ITRF2014: A new release of the International Terrestrial Reference Frame modeling nonlinear station motions. J. Geophys. Res. Solid Earth, 121(8), 6109-6131.

Auriac, A., K.H. Spaans, F. Sigmundsson, A. Hooper, P. Schmidt, & B. Lund, 2013. Iceland rising: Solid Earth response to ice retreat inferred from satellite radar interferometry and viscoelastic modelling. J. Geophys. Res. 118. 1331–1344. https://doi.org/10.1002/jgrb.50082.

Árnadóttir Th., B. Lund, W. Jiang, H. Geirsson, H. Björnsson, P. Einarsson, & Th. Sigurdsson, 2009. Glacial rebound and plate spreading: Results from the first countrywide GPS observations in Iceland. Geophys. J. Int. 177(2). 691–716. https://doi.org/10.1111/j.1365-246X.2008.04059.x

Barnhoorn, A., W. van der Wal, & M.R. Drury, 2011. Upper mantle viscosity and lithospheric thickness under Iceland. J. Geodyn. 52(3-4). 260–270. https://doi.org/10.1016/j.jog.2011.01.002

Bellagamba, G., P. Schmidt, H. Geirsson, M. Parks, E. Magnússon, J. Berlart, ... & V. Drouin, 2024. Advancing Glacial Isostatic Adjustment Modelling of Iceland into the 2020's. AGU Fall Meeting, Abstract G21B-3545, Washington DC, Dec. 9-13.

Björnsson, A., K. Sæmundsson, P. Einarsson, E. Tryggvason, & K. Grönvold, 1977. Current rifting episode in north Iceland. Nature, 266, 318–323.

Cao, Y., S. Jónsson, & S. Hreinsdóttir, 2023. Iceland kinematics from InSAR. J. Geophys. Res. Solid Earth, 128, e2022JB025546.

Einarsson, P., 1991. Earthquakes and present-day tectonism in Iceland. Tectonophys. 189. 261–279.

Einarsson, P., F. Sigmundsson, I.Þ. Magnússon, 1994. A kinematic GPS-survey in Surtsey 1992. Report Raunvísindastofnun Háskólans. RH-23-94.

Einarsson, P., & B. Brandsdóttir, 2021. Seismicity of the Northern Volcanic Zone of Iceland. Front. in Earth Sci. 9:628967. https://doi.org/10.3389/feart.628967

Einarsson, Þ., 1966. Gosið í Surtsey í máli og myndum. 2. útg. Endurskoðuð (The eruption of Surtsey. in pictures and words. in Icelandic. Second ed. revised). Heimskringla. Reykjavík.

Geirsson, H., Th. Árnadóttir, C. Völksen, W. Jiang, E. Sturkell, T. Villemin, P. Einarsson, F. Sigmundsson, & R. Stefánsson, 2006. Current plate movements across the Mid-Atlantic Ridge determined from 5 years of continuous GPS measurements in Iceland. J. Geophys. Res. 111. B09407. https://doi.org/10.1029/2005JB003717

Geirsson, H., P. LaFemina, Th. Árnadóttir, E. Sturkell, F. Sigmundsson, M. Travis, P. Schmidt, B. Lund, S. Hreinsdóttir, & R. Bennett, 2012. Volcano deformation at active plate boundaries: Deep magma accumulation at Hekla volcano and plate boundary deformation in south Iceland. J. Geophys. Res. 117, B11409. https://doi.org/10.1029/2012JB009400

Geirsson, H., M.M. Parks, F. Sigmundsson, V. Drouin, B.G. Ófeigsson, C. Lanzi, Á.G. Birgisdóttir, C. Ducrocq, A. Hooper, P. Einarsson, K. Jónsdóttir, S. Hreinsdóttir, & S.H.M. Greiner, 2024. Deformation patterns of the Reykjanes Peninsula unrest

2020-2024, Iceland: evidence for interconnected neighboring volcanic system. Abstract EGU24-18235, EGU General Assembly, Vienna, 14.-19. April.

Herring, T. A., R. W. King, & S. C. McClusky, 2010. Introduction to gamit/globk. Massachusetts Institute of Technology, Cambridge, Massachusetts 400, 401.

Hreinsdóttir, S., Th. Árnadóttir, J. Decriem, H. Geirsson, A. Tryggvason, R.A. Bennett, & P. LaFemina, 2009. A complex earthquake sequence captured by the continuous GPS network in SW-Iceland. Geophys. Res. Lett. 36(12), L12309. https://doi.org/10.1029/2009GL038391

Islam, Md.T., 2016. Rheological response to tectonic and volcanic deformation in Iceland, PhD thesis, Department of Earth sciences, University of Gothenburg.

Jakobsson, S.P, 1978. Environmental factors controlling the palagonitization of the Surtsey tephra. Iceland. Bull. Geol. Soc. Denmark 27, 91–105.

Jakobsson, S.P. & J.G. Moore, 1986. Hydrothermal minerals and alteration rates at Surtsey volcano. Iceland. Geol. Soc. Am. Bull. 97, 648–659.

Jakobsson, S.P., G. Gudmundsson & J.G. Moore 2000. Geological monitoring of Surtsey, Iceland, 1967–1998. Surtsey Res. 11, 99–108.

Leshchinsky, B., M.J. Olsen, C. Mohney, M. O'Banion, M. Bunn, J. Allan, & R. McClung, 2019. Quantifying the sensitivity of progressive landslide movements to failure geometry, undercutting processes and hydrological changes. J. Geophys. Res. Earth Surface 124(2), 616–638.

Lyard, F., F. Lefèvre, T. Letellier, & O. Francis, 2006. Modelling the global ocean tides: modern insights from FES2004. Ocean Dyn. 56, 394–415.

McPhie, J., J.D.L. White, C. Gorny, M.D. Jackson, M.T. Gudmundsson, & S. Couper, 2020. Lithofacies from the 1963–1967 Surtsey eruption in SUSTAIN drill cores SE-2a, SE-2b and SE-03, Surtsey Res. 14, 19–32.

Meyer, P.S., H. Sigurdsson, & J-.G. Schilling, 1985. Petrological and geochemical variations along Iceland's neovolcanic zones. J. Geophys. Res. 90, 10043–10072.

Moore, J.G., 1982. Tidal and leveling measurements on Surtsey July–August. 1979. Surtsey Res. Prog. Rep. IX. 98–101.

Moore, J..G. & M.D. Jackson, 2020. Observations on the structure of Surtsey, Surtsey Res. 14, 33–45.

Moore, J.G., S.P. Jakobsson, & J. Hólmjárn, 1992. Subsidence of Surtsey volcano. Bull. Volcanol. 55. 17–24.

Oskarsson, N., S. Steinthorsson, & G.E. Sigvaldason, 1985. Iceland geochemical anomaly: Origin, volcanotectonics, chemical fractionation and isotope evolution of the crust. J. Geophys. Res. 107, 10,011–10,025. https://doi.org/10.1029/JB090iB12p10011

Óskarsson, B.V., K. Jónasson, G. Valsson, & J.M.C. Belart, 2020. Erosion and sedimentation in Surtsey island quantified from new DEMs. Surtsey Res. 14, 63–77. https://doi.org/10.33112/surtsey.14.5

Pagli, C., F. Sigmundsson, B. Lund, E. Sturkell, H. Geirsson, P. Einarsson, Th. Árnadóttir, & S. Hreinsdóttir, 2007. Glacio-isostatic deformation around the Vatnajokull ice cap. Iceland. induced by recent climate warming: GPS observations and finite element modelling. J. Geophys. Res. 112(B8). 1–12.

Parks, M., V. Drouin, F. Sigmundsson, et al., 2025. 2023–2024 inflation-deflation cycles at Svartsengi and repeated dike injections and eruptions at the Sundhnúkur crater row, Reykjanes Peninsula, Iceland. Earth Planet. Sci. Lett. 658, 119324.

Perez, V., K. Jónasson, L. Ásbjörnsdóttir, & M.T. Gudmundsson, 2022. Fifty Year Evolution of Thermal Manifestations at Surtsey Volcano, 1968-2018. Surtsey Res. 15, 127–139.

Ranalli, G., 1987. Rheology of the Earth: Deformation and Flow processes in Geophysics and Geodynamics. Allen & Unwin. Boston. USA.

Sayyadi, S., M.T. Gudmundsson, J.D.L. White, T. Jónsson M.C. Brown, & M.D. Jackson, 2024. Internal structure of the volcanic island of Surtsey and surroundings: Constraints from a dense aeromagnetic survey. J. Volcanol. Geotherm. Res. 451, 108096, https://doi.org/10.1016/j.jvolgeores.2024.108096

Sayyadi, S., P. Einarsson, & M.T. Gudmundsson, 2021. Seismic activity associated with the 1963–1967 Surtsey eruption off the coast of South Iceland. Bull. Volcanol. 83(8), 54.

Sayyadi, S., M.T. Gudmundsson, & P. Einarsson, 2022. Volcanic tremor associated with the Surtsey eruption of 1963–1967. Jökull 72, 21-34.

Sclater, J.G. & P.A.F. Christi, 1980. Continental stretching: an explanation of the post-mid-Cretaceous subsidence of the central North Sea Basin. J. Geophys. Res. 85(B7). 3711–3739.

Sigmarsson, O., 2013. Constraints on primitive magma genesis and magma transfer time at Surtsey Volcano. Iceland. from U-series disequilibrium. Surtsey 50th Anniversary Conference. Reykjavík 2013. Programme and Abstracts. p. 72. Surtsey Research Society.

Stevens, N.F., G. Wadge, C.A. Williams, J.G. Morley, J-.P. Muller, J.B. Murray, & M. Upton, 2001. Surface movements of emplaced lava flows measured by synthetic aperture radar interferometry. J. Geophys. Res. 106(B6), 11293–11313.

Sturkell, E., P. Einarsson, H. Geirsson, E. Tryggvason, J.G. Moore, & R. Ólafsdóttir, 2009. Precision levelling and geodetic GPS observations performed on Surtsey between 1967 and 2002. Surtsey Res. 12. 39–47.

Thorarinsson, S., Th. Einarsson, G. Sigvaldason, & G. Eliasson, 1964. The submarine eruption off the Vestmann Islands 1963–64. a preliminary report. Bull. Volcanol. 27. 1–11.

Thorarinsson, S., 1965. The Surtsey eruption: Course of events and the development of the new island. Surtsey Res. Progr. Rep. I: 51-55.

Thorarinsson, S., 1967. The Surtsey eruption and related scientific work. Polar Rec. 13. 571–578.

Thors, K. & S.P. Jakobsson, 1982. Two seismic reflection profiles from the vicinity of Surtsey. Iceland. Surtsey Res. Progr. Rep. IX. 149–151.

Tryggvason, E., 1968. Result of precision levelling in Surtsey. Surtsey Res. Prog. Rep. IV. 149–158.

Tryggvason, E., 1972. Precision levelling in Surtsey. Surtsey Res Progr. Rep. VI. 158–162.

Tryggvason, E., 1994. Surface deformation at the Krafla volcano, North Iceland, 1982–1992. Bull. Volcanol. 56(2), 98-107.

Turcotte, D.L. & G. Schubert, 2002. Geodynamics. Second ed.. Cambridge University Press. Cambridge. UK.

Þórarinsson, S., 1964. Surtsey. Eyjan nýja á Atlantshafi. (Surtsey. The new island in the North Atlantic. in Icelandic). Almenna Bókafélagið. Reykjavík.

Þórarinsson, S., 1965. Neðansjávargos við Ísland (Submarine eruptions off Iceland. in Icelandic). Náttúrufræðingurinn 35. 49–74.

Þórarinsson, S., 1966. Sitt af hverju um Surtseyjargosið (Bits and pieces on the Surtsey eruption. in Icelandic). Náttúrufræðingurinn 35. 153–181.

Þórarinsson, S., 1969. Síðustu þættir Eyjaelda (The last phases of the Surtsey eruption. in Icelandic). Náttúrufræðingurinn 38. 113–135.

Weaver, J., G.H. Eggertsson, J.E.P. Utley, P. A. Wallace, A. Lamur, J. E. Kendrick, H. Tuffen, S.H. Markússon, & Y. Lavallée, 2020. Thermal Liability of Hyaloclastite in the Krafla Geothermal Reservoir, Iceland: The Impact of Phyllosilicates on Permeability and Rock Strength. Geofluids. https://doi.org/10.1155/2020/9057193

Wu, P., 1992. Deformation of an incompressible viscoelastic flat Earth with power-law creep: a finite element approach. Geophys. J. Int. 108. 35–51.